Synthesis and Photochemical Applications of Processable Polymers Enclosing Photoluminescent Carbon Quantum Dots

Dario Mosconi,[†] Daniela Mazzier,[†] Simone Silvestrini,[†] Alberto Privitera,[†] Carla Marega,[†] Lorenzo Franco,[†,‡] and Alessandro Moretto*[,†,§]

[†]Department of Chemical Sciences, University of Padova, Via Marzolo 1, 35131 Padova, Italy, [‡]Polo Fotovoltaico Veneto, University of Padova, Via Trasea 7, 35125 Padova, Italy, and [§]Institute of Biomolecular Chemistry, Padova Unit, CNR, Via Marzolo 1, 35131 Padova, Italy

ABSTRACT Herein, we propose convenient routes to produce hybrid-polymers that covalently enclosed, or confined, N-doped carbon quantum dots (CQDs). We focus our attention on polyamide, polyurea–urethane, polyester, and polymethylmetacrylate polymers, some of the most common resources used to create everyday materials. These hybrid materials can be easily prepared and processed to obtain macroscopic objects of different shapes, *i.e.*, fibers, transparent sheets, and bulky forms, where the characteristic luminescence properties of the native N-doped CQDs are preserved. More importantly we explore the potential use of these hybrid composites to achieve photochemical reactions as those of photoreduction of silver ions to silver nanoparticles (under UV-light), the selective photo-oxidation of benzylalcohol to the benzaldehyde (under vis-light), and the photocatalytic generation of H_2 (under UV-light).

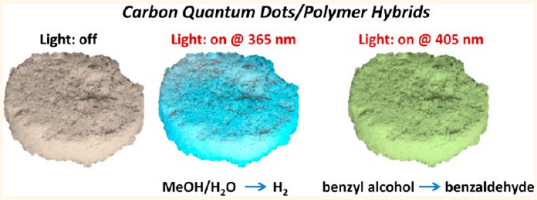

KEYWORDS: carbon nanostructures · carbon quantum dots · photoluminescence · photocatalysis · polymers

Carbon-based nanostructures are currently the center of much of the discussion in nanotechnology.[1] This class of compounds embraces a variety of carbon allotropes, different from the well-known pristine diamond and graphite, with a large number of shapes and sizes. While the popularity of carbon nanostructures to a large extent is due to fullerenes and nanotubes, other members of the nanocarbon family are also attracting gradually increasing attention.[2] Structures, properties, and numerous applications of nanostructured graphite, which belongs to a broad group of the so-called new carbon materials, have been recently proposed. Among them, carbon quantum dots (CQDs) represent a fascinating class of water-soluble carbon nanostructures, characterized by discrete, quasi-circular shapes with diameters up to 10 nm.[3−6] CQDs are nontoxic[7] carbon nanostructures that show peculiar photoluminescence (PL) properties, such as multicolor emission that varies with the excitation wavelength.[8] They have also been suggested as interesting candidates for sensing, bioimaging, and, in general, for applications where the size, cost, and biocompatibility of the label are critical issues.[9−14] The development of new types of CQDs-based materials will allow control of the fundamental properties of materials through size/shape effects, which will further allow new devices to be developed with distinctive properties and functions for numerous applications. In this connection, many interesting phenomena are expected, thanks to their remarkable quantum-confinement and edge effects.

We recently reported the bottom-up fabrication of star-shaped hybrid structures containing poly benzyl-L-glutamate (PBLG) chains prolonging outward from a CQD core.[15] In particular we started by the microwave-assisted hydrothermal synthesis of CQDs, by using arginine (Arg) and ethylenediamine, to obtain highly luminescent N-doped and amino-terminated CQDs. The combination of X-ray photoelectron spectroscopy and elemental analysis allowed for a quantitative chemical characterization of the N-doped CQDs, an aspect that has been seldom addressed to before.

* Address correspondence to alessandro.moretto.1@unipd.it.

Received for review January 15, 2015 and accepted March 15, 2015.

Published online March 15, 2015
10.1021/acsnano.5b00319

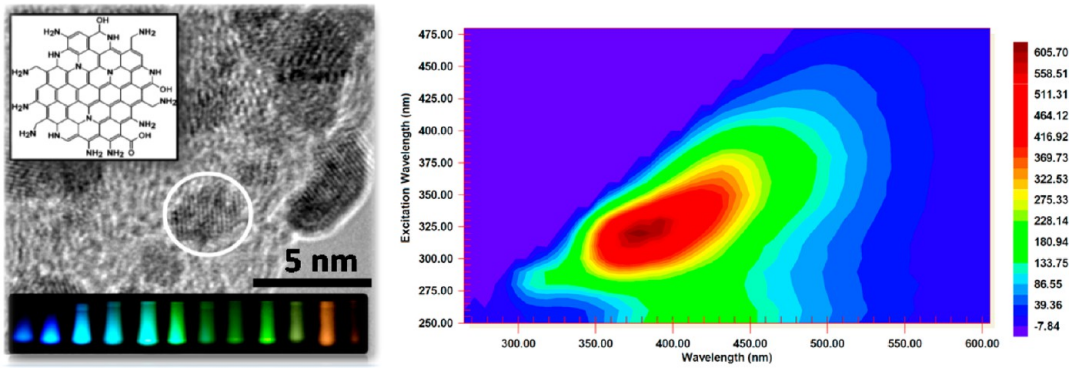

Figure 1. Left: HR-TEM image and (upper inset) the proposed chemical structure of N-doped CQDs. Lower inset: The multicolor emission of a water solution of N-doped CQDs. Right: Emission spectra of N-doped CQDs recorded in a water solution under different excitation wavelengths.

These results have open new opportunities for the in-depth synthesis and application of an emerging class of N-doped CQD-hybrids nanomaterials. In particular, once we find the type and number of functional surface groups, we could use a "molecular" approach to perform chemical reactions like polymerizations, in which N-doped CQDs can act like branching monomers.

In this work we address our attention to polyamide, polyurea–urethane, polyester, and polymethylmetacrylate (PMMA) polymers since they represent a large part of our everyday lives and they can be found in hundreds of different products. Thus, in this study we describe synthetic and processing protocols of these polymer/N-doped CQD hybrids and, more importantly, we explore their applications by studying optical, photocatalytic, and magnetic properties[3,16,17] thanks to the combination of several spectroscopic techniques such as fluorescence emission spectroscopy and electron paramagnetic resonance (EPR).

RESULTS AND DISCUSSION

As previously described, we made use of highly photoluminescent (up to 18% of quantum yield, determined by the integrating sphere method) N-doped and amino terminated-CQDs, which were obtained on large scale *via* a slight modification (see SI) of our reported microwave-assisted hydrothermal protocol, starting from a mixture of Arg and 1,2-ethylenediamine.[15] The proposed chemical structure, the high resolution transmission electron microscopy (HR-TEM) image, and the photoluminescence spectra in water of the N-doped CQDs are shown in Figure 1.

By this method, we obtain similar (in term quantum yields and nanoparticles size distribution) N-doped CQDs as those previously reported by us, but in much higher, gram-scale yield.

Nylon-6,6/N-Doped CQDs Hybrids (Polyamide). We also focus our study on the covalent inclusion of N-doped CQDs in polymeric materials.[18] To this aim, we considered the possibility to synthesize nylon-like cross-linked fibers from 1,6-hexamethylene-diamine, sebacoyl chloride, and our amino-terminated CQDs. We followed the two-phase polymerization (hexane/water) process, which allows formation of a pale-yellow material after washing-purification and dried-up steps (Figure 2 and SI).

Subsequently, the bulk material was electrospun from a formic acid solution, giving fibers.[19] We compared pure nylon electrospun fibers with electrospun fibers obtained from hybrid samples composed by three different amounts of N-doped CQDs (5, 50, and 100 w/w %, respectively, referred to 1,6-hexamethylene-diamine). As shown in Figure 2A, pure electrospun nylon fibers are characterized by almost regular and homogeneous filaments. Addition of different amounts of N-doped CQDs allowed formation of cross-linked electrospun fibers in all of the examined samples as detected by scanning electron microscopy (SEM) (Figure 2B–D). In these cases, the electrospun fibers displayed different morphologies. According to the increasing amounts of N-doped CQDs, larger fibers were obtained from the cross-link reactions that involved N-doped CQDs.

The sample that contained 100 w/w % (referred to 1,6-hexamethylene-diamine) of N-doped CQDs electrospun fibers was further examined by TEM (Figure 2E). This analysis shows in detail the cross-linked network imposed by N-doped CQDs to the polyamide fibers that generates large strips, in accord with the relative SEM results. Finally, the PL exhibited by the electrospun fibers indicated the presence of covalently linked N-doped CQDs (Figure 2). A higher concentration of N-doped CQDs in the polymer hybrid resulted in a nonprocessable material.

Polyurea–Urethane/N-Doped CQDs Hybrid. Within the polyurea class of polymer, we focus our attention to obtain a processable, up-scalable, and PL polyurethane-urea/N-doped CQDs hybrid.[20] In this case, we made use of a freshly prepared castor oil-based branched prepolymer, terminated by three isocyanate functional groups (Figure 3) and N-doped CQDs.

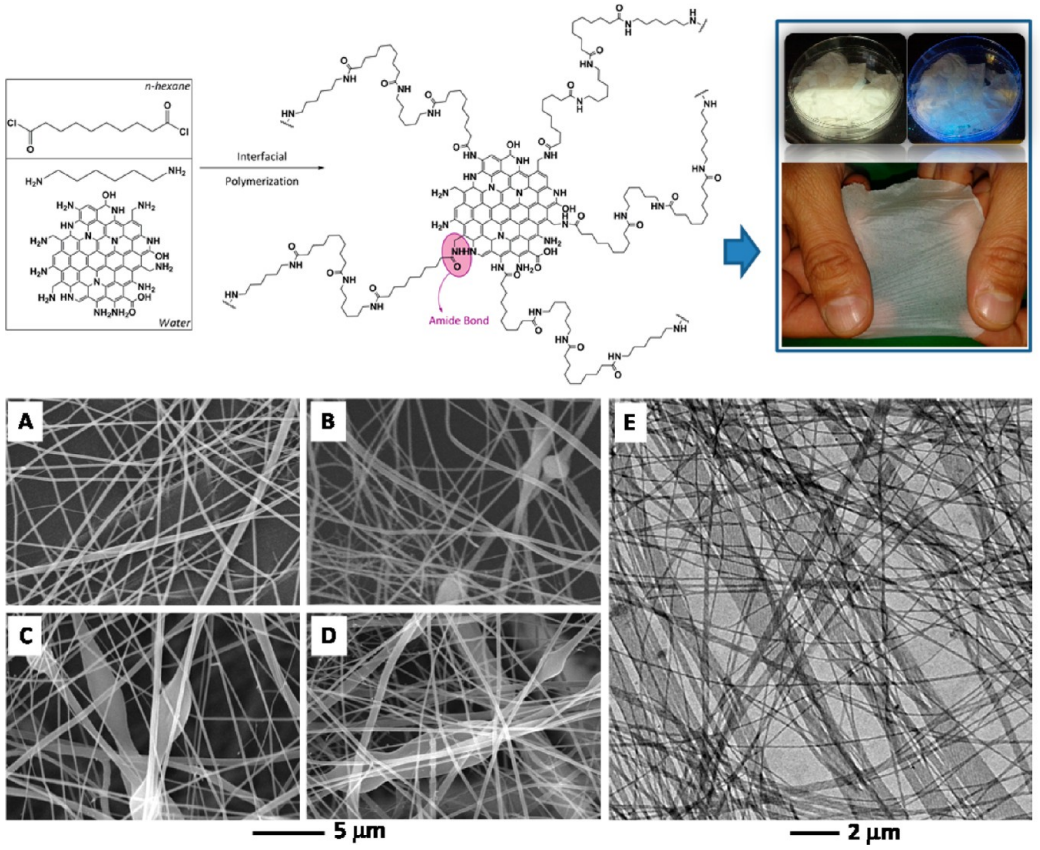

Figure 2. Top: Two-phase synthesis of nylon-6,6/N-doped CQDs hybrids and the related, macroscopic, electrospun material. Bottom: (A) SEM image of electrospun fibers from pristine nylon. (B−D) SEM image of electrospun fibers from nylon/N-doped CQDs hybrids materials obtained by use of increasing amounts of N-doped CQDs (5, 50, and 100 w/w %, respectively, referred to 1,6-hexamethylene-diamine). (E) TEM image of 100 w/w % (referred to 1,6-hexamethylene-diamine) nylon-6,6/N-doped CQD electrospun fibers.

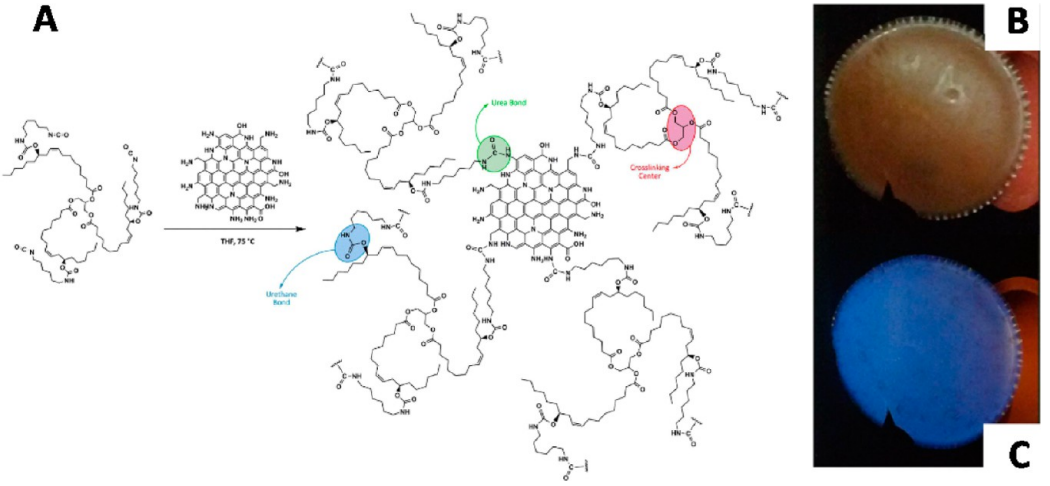

Figure 3. (A) Schematic representation of the molecular structure of the novel polyurea−urethane/N-doped CQDs hybrid. (B,C) Bulky form (hemisphere, radius = 3 cm) obtained after aging in the appropriate mold under irradiation at vis light (B) and at 365 nm (C).

Castor oil-based prepolymer was obtained by reacting pure castor oil with hexamethylene-diisocyanate under mechanical stirring while heating at 75 °C in nitrogen atmosphere. Then, dibutyltin dilaurate (DBTDL) was added to promote the prepolymer formation. After 30 min at 75 °C, CQDs dissolved in DMF/THF (tetrahydrofuran) mixture were added to the trisisocyanate solution (Figure 3). Mechanical stirring was continued for additional time to obtain a viscous mixture, which was placed in the appropriate mold. After 1−2 days of aging, the material was removed from the mold (Figure 3, right part) and characterized.

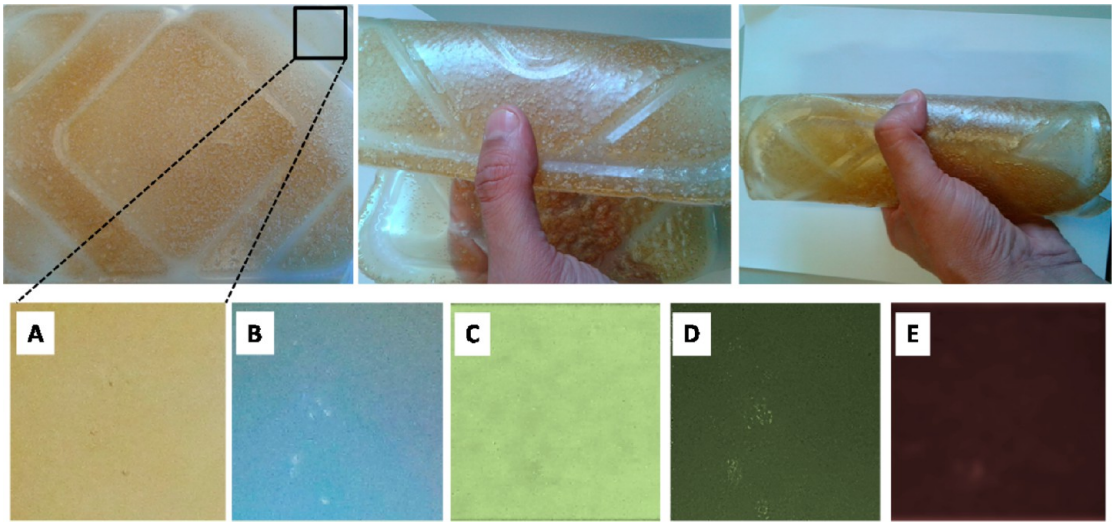

Figure 4. Upper part: Processed polymeric material (in sheet form, 30 × 50 × 0.3 cm) irradiated at different wavelengths. A = solar light, no filter; B = 405 nm, 427 nm cut-on filter; C = 465 nm, 500 nm cut-on filter; D = 500 nm, 515 nm cut-on filter; E = 585 nm, 615 nm cut-on filter.

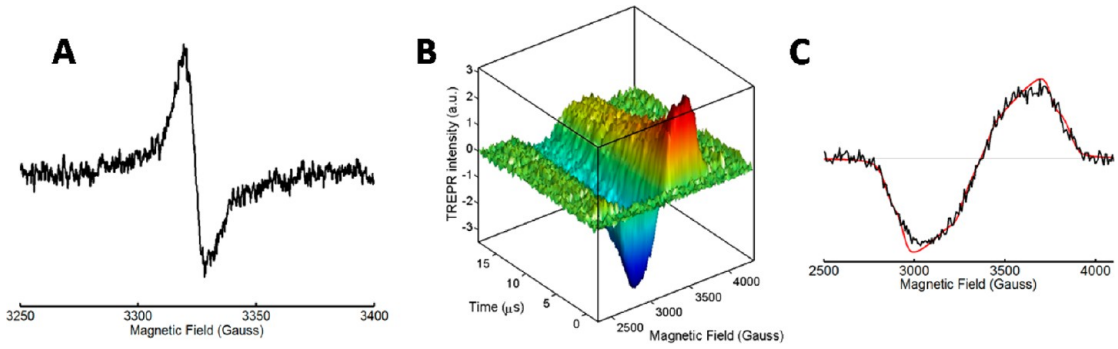

Figure 5. (A) Typical EPR spectrum of the polyurea–urethane/N-doped CQD hybrid. The spectrum shown is the difference between the spectrum recorded before sample illumination and that recorded under illumination of the sample using vis light. The difference allows elimination of the background signals arising from stable radicals. (B) Two-dimensional TREPR spectrum of the polyurea–urethane/N-doped CQDs hybrid. (C) One-dimensional TREPR spectrum taken at 0.5 μs after a vis laser pulse (black line) and best fit spectrum (red line) from which the D,E parameters of the triplet state are obtained.

We processed this polymer in a sheet form. The resulting material is shown in Figure 4 under illumination at different wavelengths, with the appropriate cut-on filters to attenuate the LED reflected light.

We applied EPR spectroscopy to check the capability of N-doped CQDs to generate paramagnetic species, such as radicals or long-lived excited triplet states, upon light absorption. Under vis-light absorption, all of the N-doped CQDs, either in solution or embedded in polymeric matrices, show photoinduced formation of radicals, as demonstrated by the appearance of weak lines in their EPR spectra (Figure 5A). The light-induced EPR spectra are composed of a single, slightly asymmetric line with a *g*-factor of about 2.003, typical of an organic radical. As the line width, *g*-factor, and microwave saturation behavior are very similar in all samples, we assign the EPR spectra to radicals localized in the N-doped CQD. The formation of radicals after light absorption could be due to photoinduced electron transfer processes from the N-doped CQD to the surrounding molecules to produce a radical cation in the carbon material and other radicals in the polymeric matrix. The latter, however, are expected to be unstable and to easily undergo fast reactions, which scavenge the radicals and prevent their EPR detection. Photoinduced electron transfer is probably not an efficient process in our samples because of the lack of a suitable electron acceptor. However, the demonstration of a photochemical activity of N-doped CQD in the polymeric matrix represents a promising result toward the application of N-doped CQD and their composites in photoactive materials where a good electron acceptor is added.

Using the time-resolved EPR technique (TREPR) with microsecond time resolution, we observed well-defined EPR spectra shortly after a vis laser pulse on samples of N-doped CQDs both in solution and in the polyurea–urethane/N-doped CQD hybrid (Figure 5B). The absence of TREPR spectra in the solid-state N-doped CQD sample (powder) can be attributed to

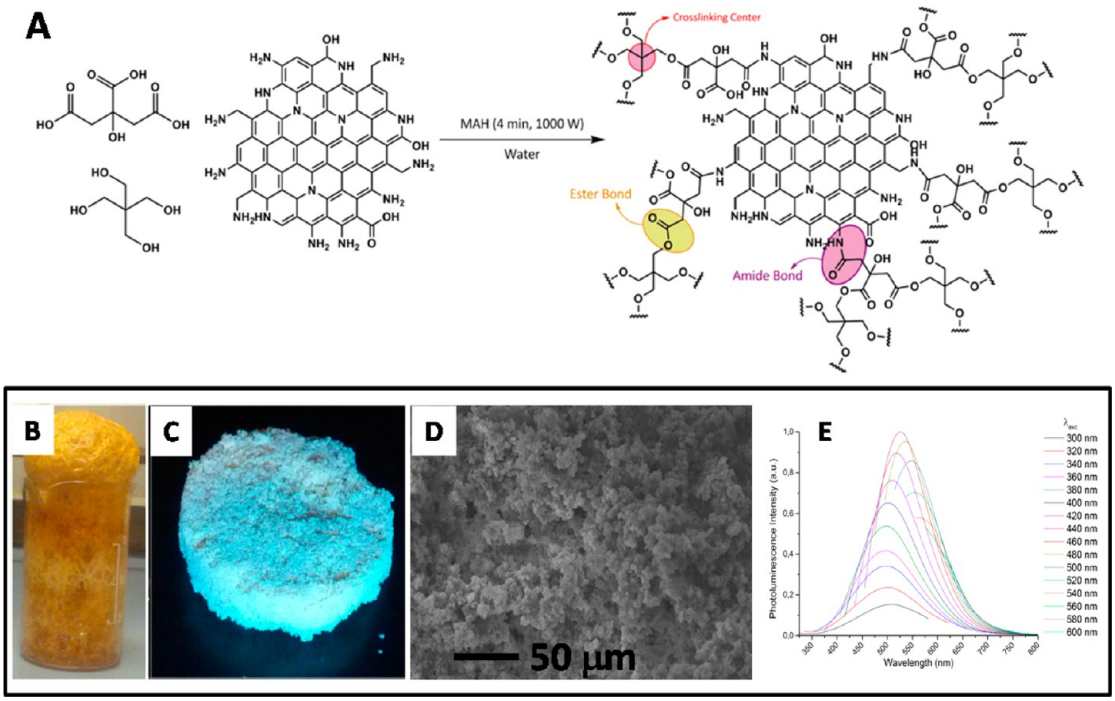

Figure 6. (A) Schematic representation of the molecular structure of the novel polyester–amide/N-doped CQDs hybrid. Lower part. (B) Polyester–amide/N-doped CQDs hybrid material in its hard and porous form. (C) Bulk material under UV light. (D) SEM image showing the porous polyester–amide/N-doped CQDs matrix. (E) Solid-state PL spectra of the polyester–amide/N-doped CQD hybrid material.

efficient quenching of the excited states promoted by intermolecular interactions. The TREPR spectra obtained in the polyurea–urethane/N-doped CQD hybrid can be assigned to the molecular excited triplet state of the N-doped CQDs, whose decay time is about 20 μs at low temperature (T = 130 K). From spectral simulation (Figure 5C) we could obtain the parameters D and E, which define the magnetic dipolar interaction between the two unpaired electrons of the triplet state.[21] In particular, the D value, related to the mean distance between the electrons in the excited state, provides an estimate of the spatial extension of the excited state wave function. The value obtained (D = 1430 MHz) is comparable with those of aromatic or aza-aromatic systems with 4–5 condensed rings (*e.g.*, pentacene, D = 1390 MHz; porphyrin, D = 1310 MHz).[22] This observation suggests that the long-living triplet excited state is confined in only a small part of the extended N-doped CQD structure. Indeed, from the size distribution of our N-doped CQDs we found an average diameter of 2.4 nm. This value approximately corresponds to a mean surface area of 452.4 Å^2 per N-doped CQD (considering a circular disk approximation). Instead, an aromatic system like pentacene has an approximate area of 25.1 Å^2, which corresponds to the 5.6% of the total area of the N-doped CQD. The possibility that our rather strong TREPR triplet spectra originated from impurities composed of small polycyclic aromatic compounds is excluded because of the repeated washing procedure of CQDs, which eliminates most of the soluble small aromatic molecules. As a consequence, it is conceivable that a generation of multiple excitons within a single N-doped CQD takes place, thus opening the way to further photophysical processes, such as energy upconversion. Moreover, our results indicate a significant triplet state quantum yield in the N-doped CQDs, suggesting the possibility to exploit the photochemical reactivity of the excited triplet states toward oxygen in photoinduced oxidations, in photodynamic therapy, or for applications, *e.g.* in photovoltaics by inducing charge separation of electrons involved in triplet states.[23–25] Importantly, the TREPR spectra obtained in all of the polymer/N-doped CQD hybrids studied in this work (polyamide, polyurea–urethane, and polyester–amide polymers, next discussed below) are all very similar, and in all cases, the EPR signal can be assigned to the molecular excited triplet state of the N-doped CQDs.

Polyester–Amide/N-Doped CQDs Hybrid. With the aim at obtaining hard and porous materials covalently enclosing N-doped CQDs, we explored the microwave-assisted synthesis of polyester–amide polymers starting from citric acid, pentaerythritol, and N-doped CQDs.[26] Thus, following the schematic representation shown in Figure 6A, we were able to produce polyester–amide/N-doped CQDs hybrid materials in hard and porous form (shown in Figure 6B–D). Interestingly, this matrix induces a dramatic change in the PL properties of the pristine N-doped CQDs by shifting up to 100 nm, the maximum emission to the vis region (Figure 6E).

Figure 7. Left: Image of a transparent PMMA/N-doped CQD material under irradiation at vis light and at 365 nm. Right: Solid-state emission spectra of a PMMA/N-doped CQD hybrid material under different excitation wavelength.

As reported in the literature, the photoluminescence of CQDs could be quenched efficiently by electron acceptor or donor molecules in solution, namely, that photoexcited CQDs are together excellent electron donors and excellent electron acceptors, thus offering new prospects for their potential use in photocatalytic applications.[27] In this contest, we took advantage of our polyester−amide/N-doped CQDs composite to run heterogeneous photocatalysis under vis light for the "green" oxidation of benzyl alcohol to benzaldehyde. In brief, following a reported protocol applied on pristine CQDs,[28] we mixed in a quartz reactor benzyl alcohol, polyester−amide/N-doped CQDs, and hydrogen peroxide (slowly added under syringe pump) and kept the mixture under irradiation with a LED at 405 nm (see SI). This wavelength was chosen after taking into account the optical properties of our system. As noticeable from UV−vis absorption spectrum (see SI), N-doped CQDs are optically active in a range that spreads from about 200 to 450 nm, but hydrogen peroxide undergoes photolysis if irradiated with 365 nm or shorter wavelengths. Moreover, LEDs with emission at 405 nm are cheap and easy to find in commerce, and this is an important feature in the case of the scaling-up process. The reaction proceeded for 10 h, resulting in a 83% conversion and 93% selectivity (results by GC−MS and ^{1}H NMR) in accord with the reported data (the rest of the selectivity result in the production of 7% benzoic acid).[28] Moreover, from our porous polyester−amide/N-doped CQDs hybrid we were able to detect photocatalytically generated H_2 from a 2:1 solution of methanol/water.[29] Reported data were obtained by using a laser illumination set up, which allowed a two-photon process during the photocatalytic reaction to take place. To this aim, we dispersed polyester−amide/N-doped CQDs in the solvent mixture and kept it under a monochromatic (365 nm) UV-light irradiation (see SI), which was chosen to have a similar photon energy to the reference experiment. Even by using a less efficient light source, we could observe H_2 generation after placing the reactor output in a $CuSO_4$ aqueous solution. The qualitative H_2 formation (in the form of bubbles) was confirmed by precipitation of metallic copper particles, thanks to the redox reaction between H_2 and Cu^{2+} cations to give $2H^+$ and Cu(0).[30] To confirm independently the formation of H_2, we run a selective hydrogenolysis, catalyzed by Pd/C, of a fully protected amino acid derivative Z-Phe-OMe (Z = benzyloxycarbonyl; Phe = phenylalanine; OMe = methylester). Although the deprotection of the Z group was not quantitative, the formation of NH_2−Phe−OMe gives a strong evidence of the effective production of H_2 (see SI). Even if more accurate studies are needed in this area, N-doped CQDs appear to be very promising low-cost catalysts even if embedded in polymeric matrices (which can be, *i.e.*, shaped in appropriate forms). These findings open the way to new applications in the design of photocatalysis devices.

PMMA/N-Doped CQDs Hybrid. With its excellent UV resistance and clarity, high gloss, scratch resistance, and superior outdoor weatherability with respect to glass, a PMMA film is turning out to be an ideal candidate as a support for solar cells. We decided to dope PMMA by adding different amounts of N-doped CQDs *via* noncovalent embedding in the already formed polymer. Starting from a solution of PMMA (350 000 Da) in dichloromethane (DCM), we prepared a set of samples with different PMMA/CQD ratios by varying the relative amount of N-doped CQDs. These N-doped CQDs are well soluble in water, MeOH, and DMF, but mostly insoluble in apolar organic solvents. In particular, when added to a DCM solution, they precipitate immediately. We found that tetraethylene glycol is able to complex N-doped CQDs with a similar mechanism as that proposed for polyethylene glycol (PEG), which is reported to solubilize CQDs in organic media.[31] Thus, N-doped CQDs were first dissolved in tetraethylene glycol with the help of the sonication procedure at 60 °C. This protocol allowed to obtain a dark and homogeneous solution, which was later on diluted by use of DCM under vigorous stirring to obtain a tinted, clear, and strongly photoluminescent DCM solution of CQDs. This last solution was subsequently combined with a

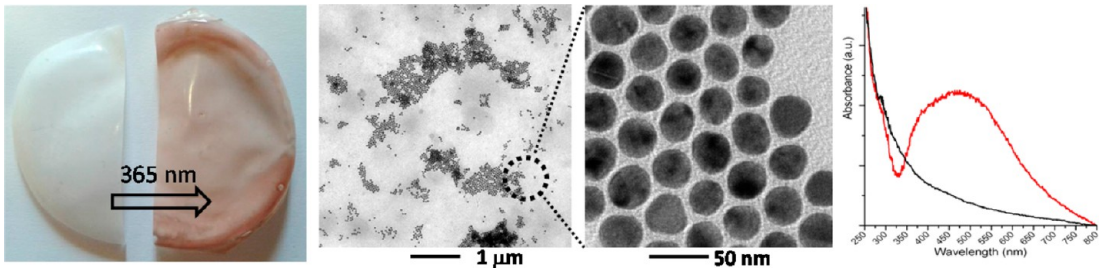

Figure 8. Left: PMMA/Ag/N-doped CQDs material prior (white) and after (pink/red) irradiation at 365 nm. This sample is opaque because of the silver nitrate saturation, which is necessary to emphasize the chromatic change caused by photoreduction. Center: TEM images of an inner layer of PMMA/AgNPs/N-doped CQDs (diluted polymer in $AgNO_3$) showing AgNP "islands" formed after UV-irradiation and details of the corresponding AgNPs. Right: thin-film UV−vis spectra of PMMA/AgNps/N-doped CQD materials prior (black line) and after (red line) irradiation at 365 nm.

DCM solution of PMMA (at different ratios of PMMA/N-doped CQDs) with the aim at including N-doped CQDs within PMMA polymers chains. After evaporation of the solvent, in all cases transparent, from light yellow to light brown (depending on the amount of N-doped CQDs), glassy materials were obtained. Importantly, these N-doped CQDs are homogeneously dispersed in the PMMA solution and eventually in the bulk. Thus, the typical fluorescence quenching effect occurring in CQDs at the solid state is prevented. These hybrid materials retained the characteristic mechanical property of native PMMA, combined with the specific PL property of N-doped CQDs (Figure 7).

It has been proposed that photocurrent enhancement by metal particles incorporated into or on solar cells is related to two main basic mechanisms, light scattering and near-field concentration of light. Thus, we exploited PMMA/N-doped CQD hybrid material to grow silver nanoparticles (AgNPs) in the form of "giant islands"[32] directly into to the polymeric hybrid matrix. To this aim, we exploited the electron-donating capabilities of photoexcited CQDs, which eventually enable the reduction of silver salts to the corresponding AgNPs on the surface of the CQDs themselves.[33] A THF solution of silver nitrate was directly mixed to a DCM solution of PMMA/N-doped CQDs. After evaporation of the solvent, the hybrid material was directly photoexcited with UV radiation (365 nm) over a period of 1 h. In our previous work, the same photoreduction was carried out in aqueous solution using 254 nm radiation, but in this case, a longer wavelength was indicated to minimize photon absorption of the PMMA matrix. Formation of AgNPs brought about a change in color (Figure 8). As expected, AgNPs were formed inside the hybrid polymeric matrix, as demonstrated by TEM and UV−vis absorption spectra analyses of the resulting irradiated material (Figure 8).

In particular, to recover TEM images the irradiated hybrid material was cut in thin layers, and the layers were examined independently (see SI). We found silver nanoparticles in all of the layers analyzed. These findings provided a clear evidence for the existence of reduced silver cluster islands in the interior part of the polymeric material.

CONCLUSIONS

In this work, we reported the synthesis and properties of novel processable materials (polyester−amide, polyurea−urethane, polyamide, and PMMA polymers) that enclose covalently or noncovalently linked N-doped photoluminescent CQDs. Since the PL properties of pristine N-doped CQDs are preserved in the polymeric matrix, transfer of these properties to bulk materials, following different routes, is an actual possibility. We successfully explored the potential of these hybrid composites to undergo photochemical reactions, *e.g.*, as those of photoreduction under UV light of silver ions to silver nanoparticles within the polymer matrix or the selective photo-oxidation under vis light of benzyl alcohol to benzaldehyde.

METHODS

Synthesis of Carbon Quantum Dots (N-Doped CQDs). Chlorohydrated arginine (10.2 g, 48.4 mmol) and ethylenediamine (3.56 mL, 53.3 mmol) are introduced in a 100 or 250 mL beaker containing 26.6 mL of ultrapure water. The solution was stirred at r.t. until complete dissolution of reactants, and then it was irradiated in a domestic microwave oven for 4 min at 1000 W. During this lapse of time, white-gray aqueous vapor came out from the vents of the oven. A porous black-reddish solid was obtained, and it was washed in a gooch filter with 4 × 20 mL aliquots of acetonitrile and 4 × 20 mL of diethyl ether. The solid was dried for several minutes in air and dissolved in the minimum volume of ultrapure water to obtain a dark and turbid solution, which is filtered through a cellulose syringe filter (0.45 μm cutoff). The purified solution was frozen using a bath of acetone and solid carbon dioxide ($T \approx -78$ °C) and then dried under vacuum through a lyophilization process, which brought on a brownish final compound.

Nylon-6,6/N-Doped CQDs Hybrid. A solution of 1,6-hexamethylenediamine (2.2 g, 18.9 mmol) in 25 mL of ultrapure water and a solution of Sebacoyl chloride (1.5 mL, 18.9 mmol) in 50 mL of *n*-hexane were prepared. The desired amount of N-doped CQDs (5, 50, and 100 w/w %, referred to 1,6-hexamethylene-diamine) were dissolved in the aqueous solution. The denser aqueous phase is poured in a 100 mL beaker, and the organic phase is slowly added above. A polymer filament can be extracted from

phase interface using tweezers, and then it is rolled up on a glass rod. The obtained solid was washed several times using ultrapure water and ethanol, and successively, it was dried in an oven at 100 °C for 2 h. Besides, samples were rewashed with ethanol and newly dried in oven. Electrospinning was carried out on a 15 w/w % nylon-6,6/N-doped CQDs hybrid solution, and the others were added with N-doped CQDs, in formic acid with an applied voltage of 18 kV, tip to collector distance of 20 cm, and solution flow rate of 0.003 mL/min.

Polyester–Amide/N-Doped CQDs Hybrid. Citric acid (15.4 g, 53.3 mmol), pentaerythritol (5.44 g, 40 mmol), and N-doped CQDs (1 g) were dissolved under vigorous stirring at 50 °C in 26.6 mL of ultrapure water in a 100 mL beaker. Then, the solution was irradiated for 4 min at 1000 W in a domestic microwave oven. The so-obtained polymer was removed from the beaker and washed with water and ethanol.

Polyurea–Urethane/CQDs Hybrid. Castor oil (6 g, 6.43 mmol) was placed in a three-neck flask, which was equipped with mechanical stirrer, N_2 influx, and $CaCl_2$ tube. Castor oil was heated at 75 °C in nitrogen atmosphere for 15 min. Hexamethylene-diisocyanate (3.5 mL, 21.79 mmol) was added and the mixture was left in the same conditions for an additional 15 min. Then, dibutyl-tin-dilaurate (4 μL, 0.04 w/w % on total reactants weight) was added, and the reaction was carried out for 30 min to allow the formation of the prepolymer. Meanwhile, an N-doped CQD solution (0.060 mg in 2 mL of anhydrous DMF) was prepared with the help of sonication, and successively, it was diluted with 10 mL of THF. This mixture was then mixed with the prepolymer, causing a significant lowering of viscosity. After several minutes of additional stirring, the so-obtained solution was placed in the appropriate mold, and it was allowed to age for 1–2 days.

EPR. The EPR spectra were recorded on a Bruker ER200D X-band spectrometer, equipped with a nitrogen flow cryostat for sample temperature control. EPR spectra are obtained as the difference between spectra with and without illumination of the sample. The illumination was achieved using white light from a 300 W xenon lamp. TREPR experiments were performed on a modified Bruker ER200D spectrometer, recording the EPR signal after a short laser pulse (Nd:YAG, Quantel Brilliant, 532 nm, 5 ns) with a LeCroy LT344 digital oscilloscope. At each magnetic field position, an average of about 200 transient signals was usually recorded. EPR spectral simulations were carried out using the Matlab toolbox Easyspin.

Conflict of Interest: The authors declare no competing financial interest.

Supporting Information Available: Additional information about synthesis, chemical characterizations, photochemical behavior, and photocatalytic activity of the hybrid materials. This material is available free of charge *via* the Internet at http://pubs.acs.org.

Acknowledgment. Financial support from the University of Padova (PRAT C91 J11003560001) and by Regione del Veneto-Polo Fotovoltaico Veneto (SMUPR no. 4148) are gratefully acknowledged.

REFERENCES AND NOTES

1. Balasubramanian, K.; Kern, K. 25th Anniversary Article: Label-Free Electrical Biodetection Using Carbon Nanostructures. *Adv. Mater.* **2014**, *26*, 1154–1175.
2. Lahiri, I.; Das, S.; Kang, C.; Choi, W. Application of Carbon Nanostructures-Energy to Electronics. *JOM* **2011**, *63*, 70–76.
3. Wang, Y.; Hu, A. Carbon Quantum Dots: Synthesis, Properties and Applications. *J. Mater. Chem. C* **2014**, *2*, 6921–6939.
4. Lim, S. Y.; Shen, W.; Gao, Z. Carbon Quantum Dots and Their Applications. *Chem. Soc. Rev.* **2015**, *44*, 362–381.
5. Bacon, M.; Bradley, S. J.; Nann, T. Graphene Quantum Dots. *Part. Part. Syst. Charact.* **2014**, *31*, 415–428.
6. Baker, S. N.; Baker, G. A. Luminescent Carbon Nanodots: Emergent Nanolights. *Angew. Chem., Int. Ed.* **2010**, *49*, 6726–6744.
7. Sk, M. P.; Jaiswal, A.; Paul, A.; Ghosh, S. S.; Chattopadhyay, A. Presence of Amorphous Carbon Nanoparticles in Food Caramels. *Sci. Rep.* **2012**, *2*.
8. Wang, L.; Zhu, S. J.; Wang, H. Y.; Qu, S. N.; Zhang, Y. L.; Zhang, J. H.; Chen, Q. D.; Xu, H. L.; Han, W.; Yang, B.; et al. Common Origin of Green Luminescence in Carbon Nanodots and Graphene Quantum Dots. *ACS Nano* **2014**, *8*, 2541–2547.
9. Li, X.; Zhang, S.; Kulinich, S. A.; Liu, Y.; Zeng, H. Engineering Surface States of Carbon Dots to Achieve Controllable Luminescence for Solid-Luminescent Composites and Sensitive Be^{2+} Detection. *Sci. Rep.* **2014**, *4*, 4976.
10. Puvvada, N.; Kumar, B. N. P.; Konar, S.; Kalita, H.; Mandal, M.; Pathak, A. Synthesis of Biocompatible Multicolor Luminescent Carbon Dots for Bioimaging Applications. *Sci. Technol. Adv. Mater.* **2012**, *13*, 045008.
11. Li, H.; He, X.; Kang, Z.; Huang, H.; Liu, Y.; Liu, J.; Lian, S.; Tsang, C. H.; Yang, X.; Lee, S. T. Water-Soluble Fluorescent Carbon Quantum Dots and Photocatalyst Design. *Angew. Chem., Int. Ed.* **2010**, *49*, 4430–4434.
12. Zhu, S.; Meng, Q.; Wang, L.; Zhang, J.; Song, Y.; Jin, H.; Zhang, K.; Sun, H.; Wang, H.; Yang, B. Highly Photoluminescent Carbon Dots for Multicolor Patterning, Sensors, and Bioimaging. *Angew. Chem., Int. Ed.* **2013**, *52*, 3953–3957.
13. Zhu, S.; Zhang, J.; Tang, S.; Qiao, C.; Wang, L.; Wang, H.; Liu, X.; Li, B.; Li, Y.; Yu, W.; et al. Surface Chemistry Routes to Modulate the Photoluminescence of Graphene Quantum Dots: From Fluorescence Mechanism to Up-Conversion Bioimaging Applications. *Adv. Funct. Mater.* **2012**, *22*, 4732–4740.
14. LeCroy, G. E.; Sonkar, S. K.; Yang, F.; Veca, L. M.; Wang, P.; Tackett, K. N.; Yu, J. J.; Vasile, E.; Qian, H.; Liu, Y.; et al. Toward Structurally Defined Carbon Dots as Ultracompact Fluorescent Probes. *ACS Nano* **2014**, *8*, 4522–4529.
15. Mazzier, D.; Favaro, M.; Agnoli, S.; Silvestrini, S.; Granozzi, G.; Maggini, M.; Moretto, A. Synthesis of Luminescent 3D Microstructures Formed by Carbon Quantum Dots and Their Self-Assembly Properties. *Chem. Commun.* **2014**, *50*, 6592–6595.
16. Liu, R.; Huang, H.; Li, H.; Liu, Y.; Zhong, J.; Li, Y.; Zhang, S.; Kang, Z. Metal Nanoparticle/Carbon Quantum Dot Composite as a Photocatalyst for High-Efficiency Cyclohexane Oxidation. *ACS Catal.* **2014**, *4*, 328–336.
17. Yang, Y.; Liu, J.; Han, Y.; Huang, H.; Liu, N.; Liu, Y.; Kang, Z. Porous Cobalt, Nitrogen-Codoped Carbon Nanostructures from Carbon Quantum Dots and VB12 and their Catalytic Properties for Oxygen Reduction. *Phys. Chem. Chem. Phys.* **2014**, *16*, 25350–25357.
18. Zhang, P.; Li, W.; Zhai, X.; Liu, C.; Dai, L.; Liu, W. A. Facile and Versatile Approach to Biocompatible "Fluorescent Polymers" from Polymerizable Carbon Nanodots. *Chem. Commun.* **2012**, *48*, 10431–10433.
19. Chun, I.; Reneker, D. H. Nanometre Diameter Fibres of Polymer, Produced by Electrospinning. *Nanotechnology* **1996**, *7*, 216.
20. Rekondo, A.; Martin, R.; Ruiz de Luzuriaga, A.; Cabañero, G. Grande, H. J.; Odriozola, I. Catalyst-Free Room-Temperature Self-Healing Elastomers Based on Aromatic Disulfide Metathesis. *Mater. Horiz.* **2014**, *1*, 237–240.
21. Weil, J. A.; Bolton, J. R. *Electron Paramagnetic Resonance: Elementary Theory and Practical Applications*, 2nd ed.; Wiley: Hoboken NJ, 2007.
22. Montalti, M.; Credi, A.; Prodi, L.; Gandolfi, M. T. *Handbook Of Photochemistry*, 3rd ed.; CRC Press: Boca Raton FL, 2006.
23. Li, Y.; Hu, Y.; Zhao, Y.; Shi, G.; Deng, L.; Hou, Y.; Qu, L. An Electrochemical Avenue to Green-Luminescent Graphene Quantum Dots as Potential Electron-Acceptors for Photovoltaics. *Adv. Mater.* **2011**, *23*, 776–780.
24. Kim, J. K.; Park, M. J.; Kim, S. J.; Wang, D. H.; Cho, S. P.; Bae, S.; Park, J. H.; Hong, B. H. Balancing Light Absorptivity and Carrier Conductivity of Graphene Quantum Dots for High-Efficiency Bulk Heterojunction Solar Cells. *ACS Nano* **2013**, *7*, 7207–7212.
25. Huang, J. J.; Zhong, Z. F.; Rong, M. Z.; Zhou, X.; Chen, X. D. An Easy Approach of Preparing Strongly Luminescent

Carbon Dots and Their Polymer Based Composites for Enhancing Solar Cell Efficiency. *Carbon* **2014**, *70*, 190–198.
26. Tisserat, B.; O'Kuru, R. H.; Hwang, H.; Mohamed, A. A.; Holser, R. Glycerol Citrate Polyesters Produced Through Heating Without Catalysis. *J. Appl. Polym. Sci.* **2012**, *125*, 3429–3437.
27. Wang, X.; Cao, L.; Lu, F.; Meziani, M. J.; Li, H.; Qi, G.; Zhou, B.; Harruff, B. A.; Kermarrec, F.; Sun, Y. P. Photoinduced Electron Transfers with Carbon Dots. *Chem. Commun.* **2009**, *25*, 3774–3776.
28. Li, H.; Liu, R.; Lian, S.; Liu, Y.; Huang, H.; Kang, Z. Near-Infrared Light Controlled Photocatalytic Activity of Carbon Quantum Dots for Highly Selective Oxidation Reaction. *Nanoscale* **2013**, *5*, 3289–3297.
29. Lavorato, C.; Primo, A.; Molinari, R.; Garcia, H. N-Doped Graphene Derived From Biomass as a Visible-Light Photocatalyst for Hydrogen Generation From Water/Methanol Mixtures. *Chem.—Eur. J.* **2014**, *20*, 187–194.
30. Cao, L.; Sahu, S.; Anilkumar, P.; Bunker, C. E.; Xu, J.; Fernando, K. A.; Wang, P.; Guliants, E. A.; Tackett, K. N.; Sun, Y. P. Carbon Nanoparticles as Visible-Light Photocatalysts for Efficient CO_2 Conversion and Beyond. *J. Am. Chem. Soc.* **2011**, *133*, 4754–4757.
31. Sun, Y. P.; Zhou, B.; Lin, Y.; Wang, W.; Fernando, K. A.; Pathak, P.; Meziani, M. J.; Harruff, B. A.; Wang, X.; Wang, H.; et al. Quantum-Sized Carbon Dots for Bright and Colorful Photoluminescence. *J. Am. Chem. Soc.* **2006**, *128*, 7756–7757.
32. Stuart, H. R.; Hall, D. G. Island Size Effects in Nanoparticle-Enhanced Photodetectors. *Appl. Phys. Lett.* **1998**, *73*, 3815–3817.
33. Choi, H.; Ko, S.-J.; Choi, Y.; Joo, P.; Kim, T.; Lee, B. R.; Jung, J.-W.; Choi, H. J.; Cha, M.; Jeong, J.-R.; et al. Versatile Surface Plasmon Resonance of Carbon-Dot-Supported Silver Nanoparticles in Polymer Optoelectronic Devices. *Nat. Photonics* **2013**, *7*, 732–738.